AD-A031 166 AEROSPACE CORP WASHINGTON D C F/G 9/3
ON PHASE DISTORTION IN LINEAR SYSTEMS.(U)
AUG 76 R K KEENAN
UNCLASSIFIED DOT-FA71WA-2577
FAA-RD-76-156 NL

| OF |
AD
A031166

END

DATE
FILMED
11-76

Report No. FAA-RD-76-156

12

ON PHASE DISTORTION IN LINEAR SYSTEMS

R. Kenneth Keenan

August 1976
Final Report

Prepared for

U.S. DEPARTMENT OF TRANSPORTATION
FEDERAL AVIATION ADMINISTRATION
Systems Research & Development Service
Washington, D.C. 20590

NOTICE

Technical Report Documentation Page

1. Report No.	2. Government Accession No.	3. Recipient's Catalog No.
FAA-RD-76-156		

4. Title and Subtitle	5. Report Date
On Phase Distortion in Linear Systems	August 1976
	6. Performing Organization Code
	8. Performing Organization Report No.
7. Author(s) R. Kenneth Keenan	
9. Performing Organization Name and Address The Aerospace Corporation 955 L'Enfant Plaza, SW Suite 4040 Washington, D.C. 20024	10. Work Unit No. (TRAIS) 11. Contract or Grant No. DOT-FA71WA-2577
12. Sponsoring Agency Name and Address U.S. Department of Transportation Federal Aviation Administration Systems Research and Development Service Washington, D.C. 20591	13. Type of Report and Period Covered Final Report 14. Sponsoring Agency Code
15. Supplementary Notes 42 p.	

16. Abstract

This report considers the general problem of analytically defining and numerically quantifying the effects of phase distortion given a specified amplitude response. A numerical example pertinent to the AEROSAT wideband communications/navigation channel is given.

Additionally, it is shown that, for systems employing correlation detection techniques and meeting certain (practical) criteria, the effects of phase distortion can be determined in a straightforward manner. The magnitude of these effects is believed to be less than that implied by the usual effort expended in specifying satellite differential group delay, but the numerical computations to prove this point have not been carried out.

17. Key Words	18. Distribution Statement
AEROSAT Group delay Paired-echo theory Phase distortion	Document is available to the public through the National Technical Information Service, Springfield, VA 22161

19. Security Classif. (of this report)	20. Security Classif. (of this page)	21. No. of Pages	22. Price
Unclassified	Unclassified	47	

Form DOT F 1700.7 (8-72) Reproduction of completed page authorized

METRIC CONVERSION FACTORS

Approximate Conversions to Metric Measures

Symbol	When You Know	Multiply by	To Find	Symbol
	LENGTH			
in	inches	*2.5	centimeters	cm
ft	feet	30	centimeters	cm
yd	yards	0.9	meters	m
mi	miles	1.6	kilometers	km
	AREA			
in^2	square inches	6.5	square centimeters	cm^2
ft^2	square feet	0.09	square meters	m^2
yd^2	square yards	0.8	square meters	m^2
mi^2	square miles	2.6	square kilometers	km^2
	acres	0.4	hectares	ha
	MASS (weight)			
oz	ounces	28	grams	g
lb	pounds	0.45	kilograms	kg
	short tons (2000 lb)	0.9	tonnes	t
	VOLUME			
tsp	teaspoons	5	milliliters	ml
Tbsp	tablespoons	15	milliliters	ml
fl oz	fluid ounces	30	milliliters	ml
c	cups	0.24	liters	l
pt	pints	0.47	liters	l
qt	quarts	0.95	liters	l
gal	gallons	3.8	liters	l
ft^3	cubic feet	0.03	cubic meters	m^3
yd^3	cubic yards	0.76	cubic meters	m^3
	TEMPERATURE (exact)			
°F	Fahrenheit temperature	5/9 (after subtracting 32)	Celsius temperature	°C

*1 in = 2.54 (exactly). For other exact conversions and more detailed tables, see NBS Misc. Publ. 286, Units of Weights and Measures, Price $2.25, SD Catalog No. C13.10:286.

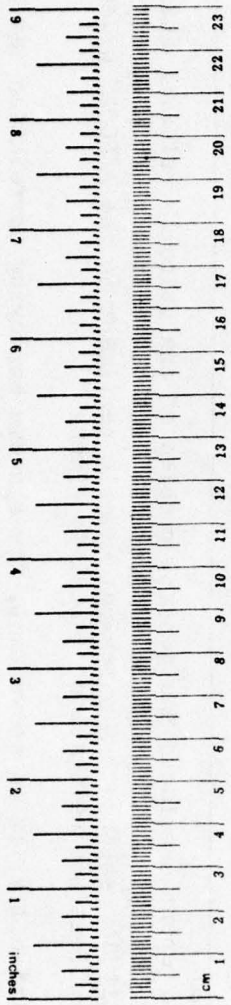

Approximate Conversions from Metric Measures

Symbol	When You Know	Multiply by	To Find	Symbol
	LENGTH			
mm	millimeters	0.04	inches	in
cm	centimeters	0.4	inches	in
m	meters	3.3	feet	ft
m	meters	1.1	yards	yd
km	kilometers	0.6	miles	mi
	AREA			
cm^2	square centimeters	0.16	square inches	in^2
m^2	square meters	1.2	square yards	yd^2
km^2	square kilometers	0.4	square miles	mi^2
ha	hectares (10,000 m^2)	2.5	acres	
	MASS (weight)			
g	grams	0.035	ounces	oz
kg	kilograms	2.2	pounds	lb
t	tonnes (1000 kg)	1.1	short tons	
	VOLUME			
ml	milliliters	0.03	fluid ounces	fl oz
l	liters	2.1	pints	pt
l	liters	1.06	quarts	qt
l	liters	0.26	gallons	gal
m^3	cubic meters	35	cubic feet	ft^3
m^3	cubic meters	1.3	cubic yards	yd^3
	TEMPERATURE (exact)			
°C	Celsius temperature	9/5 (then add 32)	Fahrenheit temperature	°F

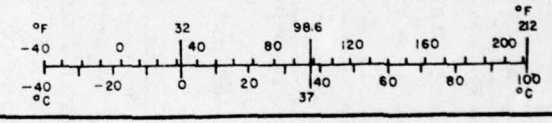

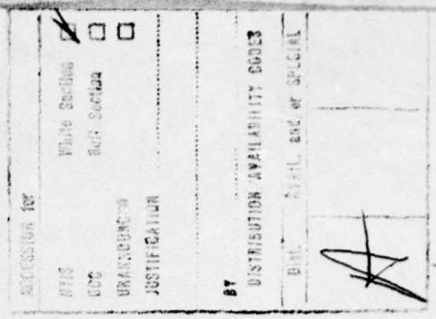

Table of Contents

1.0 INTRODUCTION

The purposes of this work are to provide an analytical basis for determining the effects of phase distortion in linear bandpass systems and to develop a model of a class of linear bandpass system functions which is useful in numerically estimating system phase $\theta(\omega)$, and its derivative, group delay $[t_{gr}(\omega)]$.

The motivation for this work stems from consideration of the Aerosat wideband channel group delay specifications in the period November-December, 1975. Two applications notes pertinent to that system are given in Sections 4.1 and 4.2.

Although the results of this work are generally applicable to lowpass and highpass system functions, primary interpretation is carried out in terms of the bandpass function shown in Figure 1.0-1.

In Section 2.0, paried-echo theory is developed. This provides a superposition-of-modulating-signal technique for determining signal distortion once the phase nonlinearities are known. In Section 3.0, the phase nonlinearities for a minimum-phase transfer function of the type shown in Figure 1.0-1 are determined.

Section 5.0 is a discussion and comparison with previous work and Section 6.0 restates the principal conclusions.

2.0 PAIRED-ECHO THEORY

The purpose of this section is to provide an analytical basis for answering the questions:

- How can the degradation of a signal due to nonlinear phase be computed?
- What is the basis for AM to PM and PM to AM conversion?

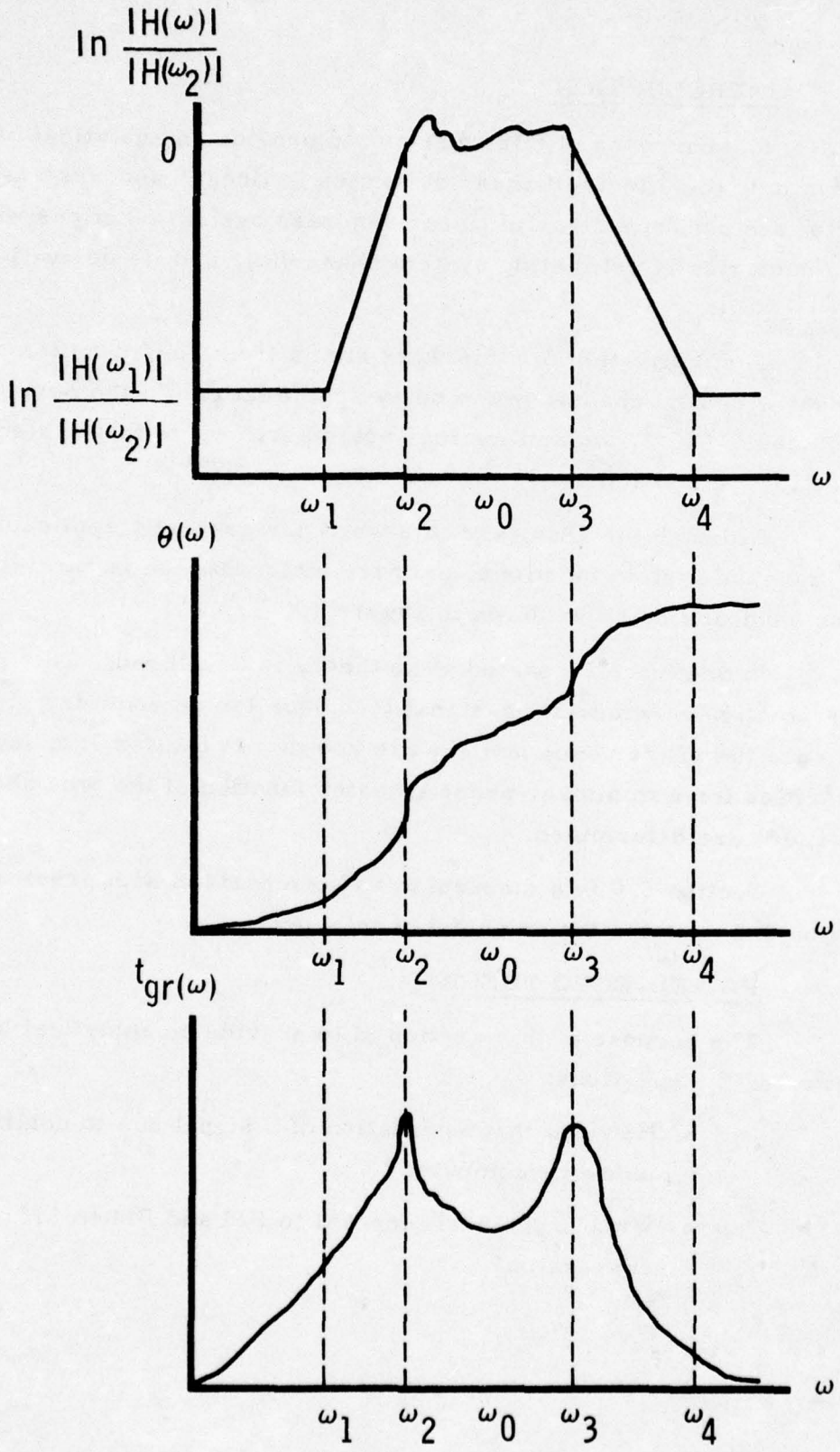

Figure 1.0-1. Bandpass Filter

2.1 The Theory

The system function indicated in Figure 1.0-1 is modeled as shown in Figure 2.1-1; the usual relationships*

$$\begin{aligned} H(\omega) &= e^{-j\theta(\omega)} |H(\omega)|, \\ Y(\omega) &= H(\omega)\, X(\omega), \\ y(t) &= h(t) \otimes x(t) \qquad (\otimes = \text{convolution operator}), \end{aligned} \tag{2.1-1}$$

hold.

The phase, $\theta(\omega)$, is expanded in a Taylor series about the center frequency, ω_o:

$$\theta(\omega) = \theta_o + (\omega - \omega_o)\, t_o + \tilde{\theta}(\omega - \omega_o), \tag{2.1-2}$$

$$\tilde{\theta}(\omega - \omega_o) = \frac{t_o'}{2!}(\omega - \omega_o)^2 + \frac{t_o''}{3!}(\omega - \omega_o)^3 + \cdots + \frac{t_o^{(n-1)}}{n!}(\omega - \omega_o)^n,$$

where

$\theta_o = \theta(\omega_o)$ = carrier delay at center frequency,

$t_o = \left.\dfrac{d\theta(\omega)}{d\omega}\right]_{\omega=\omega_o} = t_{gr}(\omega_o)$ = group delay at center frequency, and

$t_o^{(n)} = \dfrac{d^{(n)}}{d\omega^{(n)}} t_{gr}(\omega)$ = derivatives of the group delay at center frequency.

(2.1-3)

---

*The convention $H(\omega) = |H(\omega)| e^{-j\theta(\omega)}$ as opposed to $H(\omega) = |H(\omega)| e^{j\theta(\omega)}$ is chosen for convenience in dealing with the (negative phase) bandpass system function.

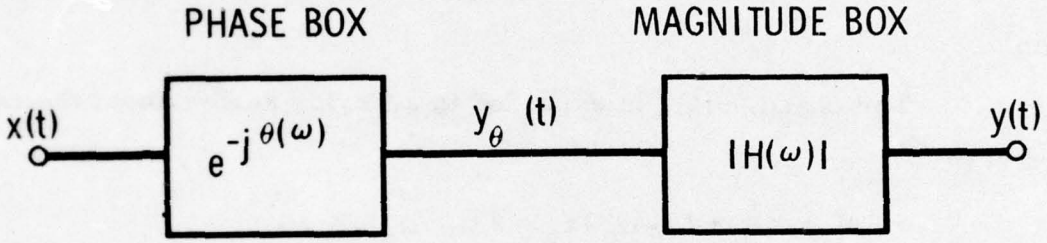

Figure 2.1-1. Model of a Linear System

In Appendix 1, it is shown that, for a $\tilde{\theta}(\omega - \omega_o)$ representable as a Fourier series in the interval (ω_2, ω_3) (only)*, the output of the system shown in Figure 2.1-1 when subjected to an input

$$x(t) = a(t)\, e^{j\omega t}, \quad a(t) \text{ real or complex} \tag{2.1-4}$$

is

$$y(t) = \tilde{y}_\theta(t) \otimes [\mathcal{F}^{-1}\,(|H(\omega)|U(\omega)], \tag{2.1-5}$$

where

$\mathcal{F}^{-1}$ = inverse Fourier transform operator and $U(\omega)$ is as shown in Figure 2.1-2.

The part $|H(\omega)|U(\omega)$ of (2.1-5) is the modification of the system output due to the magnitude response of the system, $H(\omega)$, and the interval (ω_2, ω_3) over which the Fourier expansion for $\theta(\omega - \omega_o)$ is valid. In most of what follows, attention is restricted to $\tilde{y}_\theta(t)$. Any degradation which occurs in $\tilde{y}_\theta(t)$ is, in baseband terms, simply lowpass filtered by the lowpass version of $|H(\omega)|U(\omega)$.

In Appendix 1, it is shown that

$$\tilde{y}_\theta(t) = \sum_{n=-\infty}^{\infty} c_n\, e^{j\left[\omega t - \theta_o + (\omega_o - \omega)(t_o + n\tau)\right]}\, a(t - t_o - n\tau), \tag{2.1-7}$$

where

$$\tau = \frac{2\pi}{\omega_3 - \omega_2} = \frac{1}{f_3 - f_2}, \text{ and}$$

$$c_n = \frac{1}{\omega_3 - \omega_2} \int_{\omega_2}^{\omega_3} e^{-j\left[\tilde{\theta}(\omega - \omega_o) + 2\pi n(\omega - \omega_o)(\omega_3 - \omega_2)\right]}\, d\omega. \tag{2.1-8}$$

*The Taylor then Fourier series expansion of $\tilde{\theta}(\omega - \omega_o)$ proves convenient when the properties of the Fourier coefficients are considered (Section 2.3).

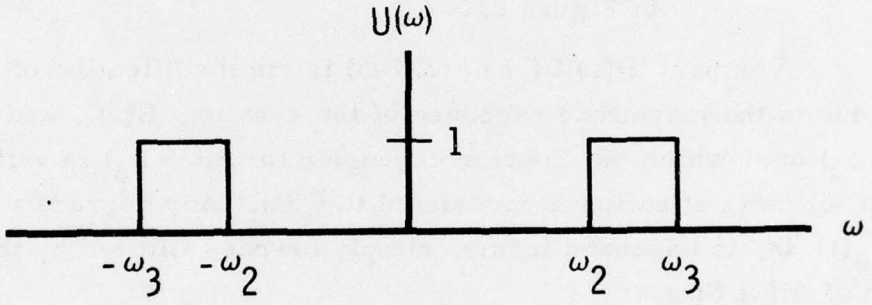

Figure 2.1-2. $U(\omega)$

When the center frequency of the input signal is equal to the center frequency of the system (i.e., $\omega = \omega_o$), (2.1-7) reduces to

$$y_\theta(t)\Big]_{\omega=\omega_o} = \sum_{n=-\infty}^{\infty} c_n \, e^{j[\omega_o t - \theta_o]} \, a(t - t_o - n\tau). \qquad (2.1\text{-}9)$$

To the extent that the interval (ω_2, ω_3) is finite, the result (2.1-5) is approximate; in practice, it can occur that tractable expansions for $H(\omega)$ are only known in some finite bandpass interval (ω_2, ω_3). Then, (2.1-5) is only that part of the output which is due to the bandpass interval. To this must be added that part of the output due to skirt response. As will be exemplified in Section 3.0, it is oftentimes convenient to separate in-band and out-of-band responses.

2.2 Heuristic Interpretation

For the purposes of initial interpretation, it is assumed that $\omega = \omega_o$ and that $a(t)$ and the c_n are real in (2.1-9). The case of a complex $a(t)$ is treated later in the present section, and the case of complex c_n is treated in Section 2.4.

In order to illustrate the effects of phase distortion, consider the following example: Let $a(t) = \pm 1$ (biphase modulation) with period 3τ and let the phase distortion, $\tilde{\theta}(\omega - \omega_o)$ be such that $c_o = 0.75$, $c_1 = 0.25$, $c_{-1} = 0.25$, $c_n = 0$, $n \neq 0, 1, -1$. The modulation present at the output of the phase box is shown in the lowest diagram of Figure 2.2-1. Clearly, this is not a replica of that at the input. Depending on the specific nature of the detector, this could cause bit errors at the receiver.

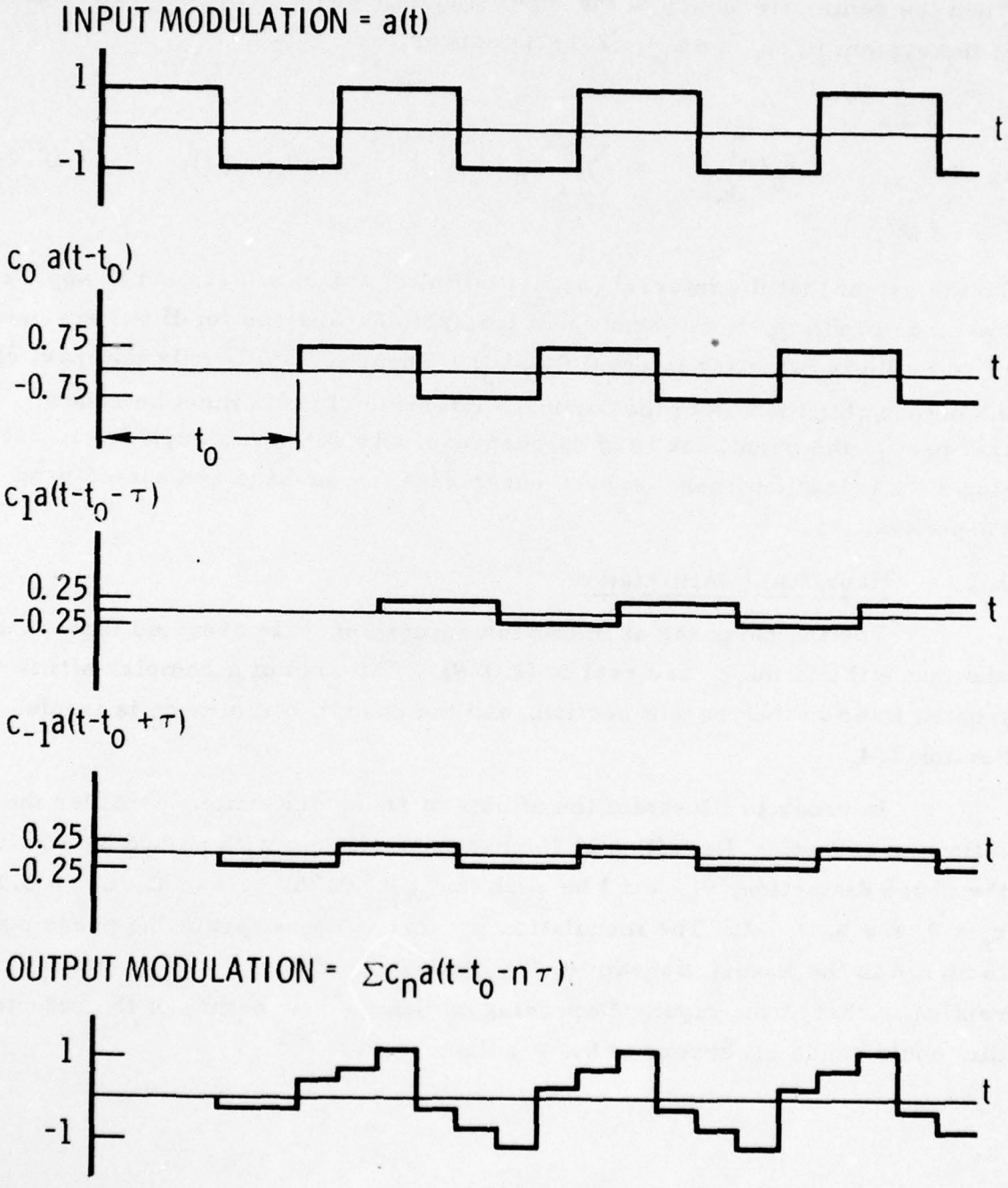

Figure 2.2-1. Distortion of a Square-Wave Modulating Function Due to Nonlinear Phase

If there was no phase distortion, i.e., if $\tilde{\theta}(\omega - \omega_o) = 0$ in (2.1-2), $c_o = 1$, $c_n = 0$, $n \neq 0$. Then, the output modulation is a delayed (by t_o) version of the input modulation, a(t) (second diagram in Figure 2.2-1 with $c_o = 1 \neq 0.75$). In the general case, however, there are an infinite number of superposed signals due to phase nonlinearity.

The above interpretation is easily extended to PM signals. Let

$$a(t) = e^{j\phi(t)} . \tag{2.2-1}$$

Then, $\tilde{y}_\theta(t)$ is, from (2.1-9),

$$y_\theta(t) = e^{j(\omega_o t - \theta_o)} \sum_{n=-\infty}^{\infty} c_n \, e^{j\phi(t-t_o-n\tau)} . \tag{2.2-2}$$

The output modulation (following the Σ sign) is still delayed by $t_o + n\tau$; in some works, group delay is called "envelope delay." In the present example, there is no varying envelope but, yet, the modulation is delayed by $t_o + n\tau$. For obvious reasons, the term "group delay" is to be preferred.

The graphical interpretation exemplified by Figure 2.2-1 is still applicable. In the PM case, one must consider both the real and imaginary parts of the output modulation.

2.3 Properties of the c_n

By the change of variable

$$\xi = 2\pi \left(\frac{\omega - \omega_o}{\omega_3 - \omega_2} \right) \tag{2.3-1}$$

in (2.1-8),

$$c_n = \frac{1}{2\pi}\int_{-\pi}^{\pi} e^{-j\left[\tilde{\theta}(K\xi)-n\xi\right]}d\xi, \qquad K = \frac{\omega_3 - \omega_2}{2\pi}$$

$$= \frac{1}{2\pi}\left[\int_{-\pi}^{\pi}\cos\left[\tilde{\theta}(K\xi) - n\xi\right]d\xi - j\int_{-\pi}^{\pi}\sin\left[\tilde{\theta}(K\xi) + n\xi\right]d\xi\right] \tag{2.3-2}$$

where, from (2.1-2),

$$\tilde{\theta}(K\xi) = \frac{t_o'}{2!}(K\xi)^2 + \frac{t_o''}{3!}(K\xi)^3 + \cdots + \frac{t_o^{(n-1)}}{n!}(K\xi)^n. \tag{2.3-3}$$

In Appendix 2, it is shown that, for any minimum-phase system which is symmetric in magnitude about ω_o with a bandwidth much less than twice the center frequency, $t_{gr}(\omega)$ is even about ω_o; i.e., if

$$|H(\omega_o + \Delta\omega)| = |H(\omega_o - \Delta\omega)|$$
$$\text{and } 2\omega_o \gg \omega_3 - \omega_2, \tag{2.3-4}$$

then

$$t_{gr}(\omega_o + \Delta\omega) = t_{gr}(\omega_o - \Delta\omega). \tag{2.3-5}$$

It follows from this result that the odd derivatives of $t_o = t_{gr}(\omega_o)$ are zero:

$$t_o^{(n)} = 0, \qquad n \text{ odd}. \tag{2.3-6}$$

Then, from (2.3-3) with $t_o^{(n)} = 0$, n odd,

$$\tilde{\theta}(-K\xi) = -\tilde{\theta}(K\xi). \tag{2.3-7}$$

That is, $\tilde{\theta}(K\xi)$ is odd. The second term of the second expression in (2.3-2) assumes the form:

$$-j \int_{-\pi}^{\pi} \sin\left[\text{odd function of } \xi\right] d\xi = 0. \tag{2.3-8}$$

Then, the c_n are real. By expanding $\cos\left[\tilde{\theta}(K\xi) - n\xi\right]$ as the sum of sin sin and cos cos terms and making use of the property (2.3-7), it is easy to show that, for the restrictions (2.3-4),

$$c_{-n} = -c_n \cong \frac{1}{2\pi} \int_{-\pi}^{\pi} \sin \tilde{\theta}(K\xi) \sin n\xi \, d\xi, \text{ real, } n \neq 0. \tag{2.3-9}$$

Now, attention is directed to another property of the c_n: convergence. Causality implies that the system cannot respond before an input is applied. In terms of the example in Figure 2.2-1, the n in the c_{-n} is bounded to a maximum of 2; otherwise, the output would occur before the input. In general,

$$c_{-n} = o \text{ for } n > \text{lowest integral value of } \frac{t_o}{\tau} \tag{2.3-10}$$

At least in the case (2.3-4), this also bounds the maximum n in c_n via (2.3-9).

Finally, attention is directed to the uniqueness of the c_n: for each choice of the interval (ω_2, ω_3), there exists a different set of c_n spaced at $\tau = 2\pi/(\omega_3 - \omega_2)$ seconds. The choice of τ is somewhat judgemental. Oftentimes, there is a tractable expansion for $H(\omega - \omega_o)$ applicable to the bandpass interval only (e.g., the 3dB or 1dB bandwidth) which will dictate the choice. It should be noted that, as the interval τ becomes larger, a larger set of the c_n have to be computed [See (2.3-10) and (2.3-9)].

2.4 A Comment on AM to PM and PM to AM Conversion

In the general (asymmetric $|H(\omega)|$) case, the c_n are complex. From a term-by-term expansion of the output (2.1-9) of the phase box involving Re c_n + jIm c_n, it is easy to show that PM is induced in an AM signal [a(t) real] and that AM is induced in a PM signal $[a(t) = e^{j\phi(t)}]$. Both effects are undesirable. Therefore, arithmetically symmetric systems [c_n real] are desirable.

By using (2.1-7) and expanding in the manner indicated above, it is easy to show that, even if $|H(\omega)|$ is symmetric, the aforementioned AM to PM and PM to AM conversion effects occur when the signal center frequency, ω, is not equal to the system center frequency, ω_o.

3.0 GROUP DELAY OF AN IDEALIZED MINIMUM-PHASE BANDPASS SYSTEM

In the writing of system specifications, the magnitude characteristics are usually considered first. These control out-of-band rejection, smoothness of the in-band response, intermodulation distortion, etc. If only voice communications with standard non-encoded AM and/or PM modulation is employed, amplitude specifications are all that is necessary, as the human ear is substantially oblivious to phase distortion. However, if digital and/or navigation signals are employed, group delay is usually considered. Oftentimes, a tradeoff must be made between phase and amplitude specifications and the cost of equalizing (i.e., making more linear) the phase characteristics.

The thrust of the present work is that of taking as given the amplitude characteristic and inferring the phase characteristic. This addresses the practical questions of, e.g.,

- How does (amplitude) skirt steepness affect group delay?
- How does in-band (amplitude) ripple affect group delay?

In the following, minimum-phase (no zeros in the right half plane) filters are considered. In practical terms, this means that unequalized filters are considered. This includes Butterworth, Tchebyshev, Elliptic function and other such filters that are normally used to meet amplitude specifications. Even if it is intended to equalize, this minimum-phase problem is generally considered first in order to assess the difficulty of designing the equalizer; most "equalized" systems are a cascade of a minimum-phase network and an "all-pass" equalizer.

Again, Figure 1.0-1 indicates the class of systems under consideration. In Section 3.1, the case of a flat in-band magnitude response is treated. Section 3.2 extends this to an arbitrary magnitude response.

3.1 Group Delay of an Idealized Minimum-Phase System Without In-Band Amplitude Distortion

The principal aim here is to restate the results of Holmes and Keenan[1] pertinent to the filter shown in Figure 1.0-1 with a flat in-band response. These will be used later in the applications notes in Section 4.0.

Holmes and Keenan show that, for the above bandpass system,

$$t_{gr}(\omega) = \frac{1}{\pi} \ln \left[\frac{|H(\omega_2)|}{|H(\omega_1)|} \right] \left[\frac{1}{\omega_2 - \omega_1} \ln \left(\frac{\omega^2 - \omega_1^2}{\omega^2 - \omega_2^2} \right) + \frac{1}{\omega_4 - \omega_3} \ln \left(\frac{\omega_4^2 - \omega^2}{\omega_3^2 - \omega^2} \right) \right], \quad \omega_2 < \omega < \omega_3. \tag{3.1-1}$$

It is also shown that, if $2\omega_o \gg (\omega_3 - \omega_2)$,

$$t_{gr}(\omega) \simeq \frac{1}{\pi} \ln \left[\frac{|H(\omega_2)|}{|H(\omega_1)|} \right] \left[\frac{1}{\omega_2 - \omega_1} \ln \left(1 + \frac{\omega_2 - \omega_1}{\omega_3 - \omega} \right) + \frac{1}{\omega_4 - \omega_3} \ln \left(1 + \frac{\omega_4 - \omega_3}{\omega_3 - \omega} \right) \right],$$

$$\omega_2 < \omega < \omega_3. \tag{3.1-2}$$

In the symmetric case $|H(\omega + \Delta\omega)| = |H(\omega - \Delta\omega)|$, (3.1-2) reduces to

$$t_{gr}(\omega) \cong \frac{1}{\pi\Omega} \ln \left[\frac{|H(\omega_2)|}{|H(\omega_1)|} \right] \ln \left[\left(1 + \frac{\Omega}{\omega - \omega_2} \right) \left(1 + \frac{\Omega}{\omega_3 - \omega} \right) \right],$$

$$\Omega = \omega_2 - \omega_1 = \omega_4 - \omega_3, \qquad \omega_2 < \omega < \omega_3. \tag{3.1-3}$$

Now, one measure of the amount of group delay distortion is

$$\Delta t_{gr} = \text{maximum group delay} - \text{minimum group delay} \tag{3.1-4}$$

From (3.1-3), this is easily shown to be

$$\Delta t_{gr} \cong \frac{1}{\pi\Omega} \ln \left[\frac{|H(\omega_2)|}{|H(\omega_1)|} \right] \ln \left[\frac{\left(1 + \frac{a}{1+K} \right) \left(1 + \frac{a}{1-K} \right)}{(1+a)^2} \right], \tag{3.1-5}$$

where

$$a = 2\Omega/(\omega_3 - \omega_2) > 0 \text{ and}$$
$$K = \text{Fraction of filter bandwidth occupied by the signal} < 1. \tag{3.1-6}$$

The case K = 1 corresponds to the signal bandwidth equal to the filter bandwidth and, due to the discontinuous slope of the magnitude characteristic occurring when the in-band response is flat in (ω_2, ω_3) in Figure 1.0-1,

infinite Δt_{gr}. In a practical approximation of the magnitude characteristic (Butterworth, Chebyshev, etc.), Δt_{gr} is not infinite. The model tends to provide estimates of Δt_{gr} which are large in comparison with those incurred in a practical realization; the closeness of the upper bounding decreases with increasing K.

3.2 The Effects of In-Band Amplitude Distortion

In this section, the work of Holmes and Keenan is extended to include the effects of an arbitrary continuous in-band amplitude function, $F(\omega - \omega_2)$. In Appendix 3, it is shown that this function can be represented as*

$$F(\omega - \omega_2) = \ln \left[\frac{|H(\omega)|}{|H(\omega_2)|}\right] = \sum_{n=1}^{\infty} b_n \sin n\pi \left(\frac{\omega - \omega_2}{\omega_3 - \omega_2}\right), \qquad (3.2\text{-}1)$$

where

$$b_n = \frac{1}{\omega_3 - \omega_2} \int_{\omega_2}^{\omega_3} F(\omega - \omega_2) \sin n\pi \left(\frac{\omega - \omega_2}{\omega_3 - \omega_2}\right) d\omega. \qquad (3.2\text{-}1a)$$

Figure 3.2-1 illustrates some special cases; all $b_n = 0$, n even, corresponds to the symmetric $|H(\omega)|$ case.

In Appendix 2, it is shown that that part of the group delay due to (arbitrary) amplitude distortion of the form (3.2-1) is

---

*$F(\omega - \omega_2)$ being expanded about ω_2 in terms of a sin function only does not restrict the eveness or oddness about ω_o, but only the continuity of $F(\omega_2)$: $F(0) = F(\omega_3)$. (3.2-1) is, then, an arbitrary but continuous function.

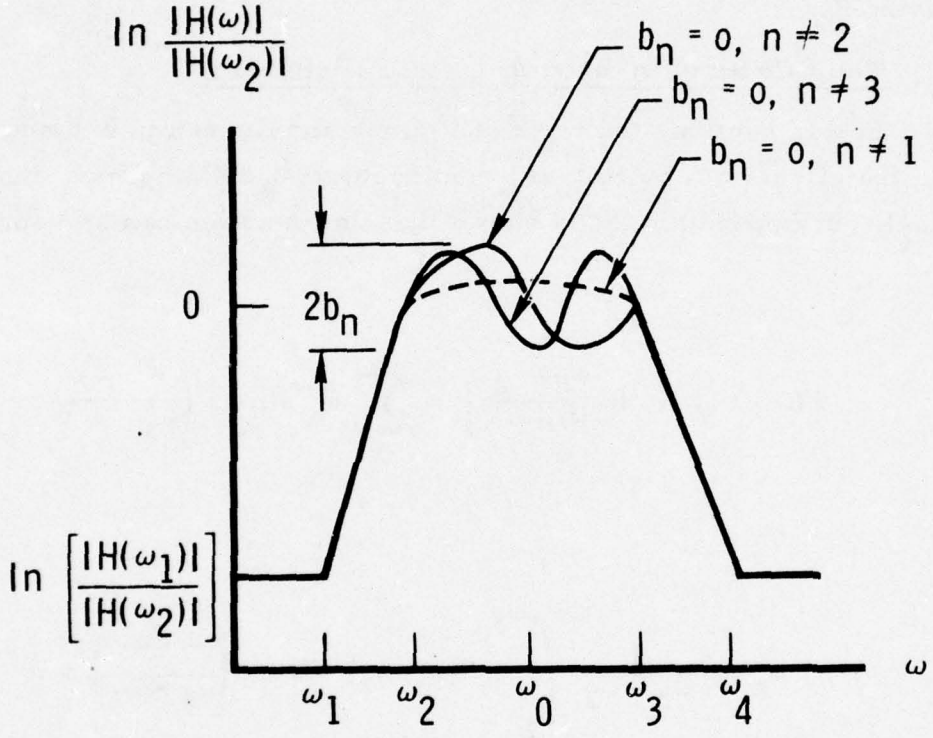

Figure 3.2-1. Special Cases of Amplitude Distortion: Ripple

$$t_{gr}(\omega_o + \Delta\omega) \cong \sum_{n=1,3,\ldots}^{\infty} \frac{(-1)^{\frac{n-1}{2}} nb_n}{\omega_3 - \omega_2} \left\{ \sin \frac{n\pi\Delta\omega}{\omega_3 - \omega_2} \left[Ci\,(a - b\Delta\omega) - Ci(a + b\Delta\omega) \right] \right.$$

$$\left. + \cos \frac{n\pi\Delta\omega}{\omega_3 - \omega_2} \left[Si\,(a - b\Delta\omega) + Si\,(a + b\Delta\omega) \right] \right|$$

$$+ \sum_{n=2,4,\ldots}^{\infty} \frac{(-1)^{\frac{n}{2}+1} nb_n}{\omega_3 - \omega_2} \left\{ \cos \frac{n\pi\Delta\omega}{\omega_3 - \omega_2} \left[Ci\,(a - b\Delta\omega) - Ci\,(a + b\Delta\omega) \right] \right.$$

$$\left. - \sin \frac{n\pi\Delta\omega}{\omega_3 - \omega_2} \left[Si\,(a - b\Delta\omega) + Si\,(a + b\Delta\omega) \right], \right| \qquad (3.2\text{-}2)$$

where the only approximation which has been made is $2\omega_o \gg (\omega_3 - \omega_2)$ and

$$a = n\pi/2,$$

$$b = n\pi/(\omega_3 - \omega_2),$$

$$Si(z) = \int_o^z \frac{\sin\lambda}{\lambda}\, d\lambda, \text{ and} \qquad (3.2\text{-}3)$$

$$Ci(z) = \int_\infty^z \frac{\cos\lambda}{\lambda}\, d\lambda.$$

In the special case of arithmetic symmetry, the terms following the second summation in (3.2-2) are zero. In the special case of the ripple indicated in Figure 3.2-1, all terms but one in (3.2-2) are zero.

The group delay incurred in the interval (ω_2, ω_3) is that in (3.2-2) plus that computed in (3.1-1).

4.0 APPLICATIONS NOTES

Applications of the foregoing theory were incurred in the course of specifying the (wideband) Aerosat satellite transponder. For a narrowband application, see Holmes and Keenan.[1]

4.1 Differential Group Delay of the Aerosat Wideband Channel

In writing a specification for the Aerosat wideband ($\approx$ 10 MHz) channel, it was desired to specify the spacecraft differential group delay in such a manner as to not force the task of equalization on the spacecraft designer; equalization (if necessary) is best carried out at the ground receiver sites. The problem, then, is to determine the group delay incurred if a minimum-phase (i.e., unequalized) filter is used to meet the satellite magnitude response requirements.

The sole constraints on the magnitude response of the satellite were that the noise bandwidth was, maximally, 10 to 12 MHz and that a signal of bandwidth between 5 and 8 MHz had to be handled with little or no amplitude degradation.

The channel characteristics were, the, of the nature shown in Figure 1.0-1 with arithmetic symmetry and a flat in-band response. In Appendix 4, it is shown that the noise bandwidth of this channel is*

$$N \cong (f_3 - f_2) + \frac{\Omega}{\ln(1000)},$$
$$\Omega = f_2 - f_1 = f_4 - f_3. \qquad (4.1\text{-}1)$$

With N fixed at 10 MHz or 12 MHz, a relationship is established between Ω and the bandwidth, $(f_3 - f_2)$. This relationship is used in (3.1-5) to obtain the results given in Figure 4.1-1.

---

*The approximation arises due to neglecting the contribution to the noise bandwidth outside the 60dB bandwidth of the filter.

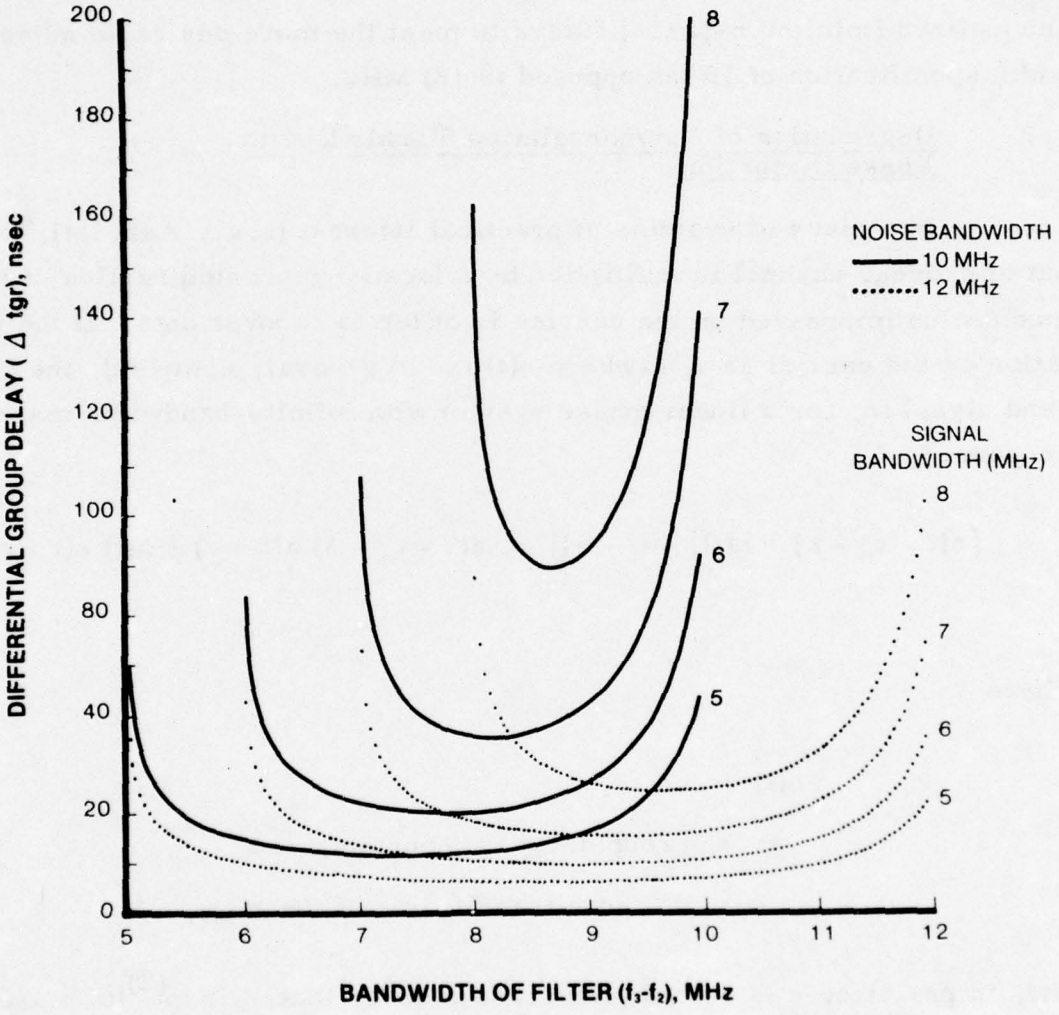

Figure 4.1-1. Differential Group Delay Incurred in an Idealized Unequalized Channel with Fixed Noise Bandwidth as a Function of the Channel Bandwidth

For the 5 MHz signal bandwidth case, it was recommended that 30 nsec Δt_{gr} be allowed and, for the 8 MHz signal bandwidth case, that a Δt_{gr} of 150 nsec be allowed. This permits the spacecraft designer to use unequalized (minimum-phase) filters to meet the more desirable noise bandwidth specification of 10 (as opposed to 12) MHz.

4.2 Degradation of Autocorrelation Signals Due to Phase Distortion

In a class of systems of practical interest (e.g., Aerosat), the output of a linear channel is multiplied by a locally-generated replica of the modulation impressed on the carrier in order to recover data. If the modulation on the carrier is a(t) (where a(t) is, in general, complex), the baseband signal is, for a linear-phase system with infinite-bandwidth magnitude response*

$$\left[a(t - t_o - \lambda) + n(t)\right]\left[a(t - \sigma)\right] = a(t - t_o - \lambda)\, a(t - \sigma) + n(t)\, a(t - \sigma), \tag{4.2-1}$$

where

$$\begin{aligned} n(t) &= \text{noise,} \\ t_o &= \text{group delay} = \text{constant, and} \\ \lambda &= \text{unknown transit time of the signal,} \end{aligned} \tag{4.2-2}$$

and, in practice, σ is varied (usually in a delay-locked loop[2]) to maximize the function

$$R_y(\sigma - t_o - \lambda) = \frac{1}{2T} \int_{-T}^{T} a(t - t_o - \lambda)\, a(t - \sigma)\, dt, \tag{4.2-3}$$

*Modification of a(t) by the finite bandwidth of the system is not under consideration here; only the degrading effects of phase nonlinearity are being considered. $|H(\omega)| = 1$ for this purpose.

where 2T is the period over which integration (integrate and dump) takes place. The maximum, $R_y(0)$, occurs when $\sigma = t_o + \lambda$. Because t_o is known a priori, determination of σ provides a measure of λ, hence the transit time of the signal and navigation and other data. If the integration period, 2T, extends over many intervals of τ (τ = 1/system bandwidth), $R_y(\sigma - t_o - \lambda)$ is a good approximation of the formal autocorrelation function of $a(t - t_o - \lambda)$.

The question arises as to the effect of nonlinear phase on the autocorrelation function of the output of the system. Consider the signal part of the output translated to baseband [$\omega_o = \theta_o = 0$ in (2.1-9)]:

$$y_\theta(t) = y(t) = c_o\, a(t - t_o - \lambda) + \sum_{\substack{n=-\infty \\ n\neq 0}}^{\infty} c_n\, a(t - t_o - \lambda - n\tau). \quad (4.2\text{-}4)$$

For the moment, assume that the system is minimum-phase and symmetric in magnitude so that $c_{-n} = -c_n$, real [See (2.3-9)]. Then, for a nonlinear phase system, the autocorrelation function of the output of the system (i.e., the output "signal") is

$$\begin{aligned} R_y(\sigma - t_o - \lambda) = {} & \frac{c_o}{2T}\int_{-T}^{T} a(t - t_o - \lambda)\, a(t - t_o - \lambda)\, dt \\ & + \sum_{n=1}^{\infty} \frac{c_n}{2T}\left[\int_{-T}^{T} a(t - t_o - \lambda - n\tau)\, a(t - t_o - \lambda - n\tau - \sigma)\, dt \right. \\ & \left. - \int_{-T}^{T} a(t - t_o - \lambda + n\tau)\, a(t - t_o - \lambda + n\tau - \sigma)\, dt\right], \end{aligned} \quad (4.2\text{-}5)$$

where the integrals following the (one-sided) Σ stem from $c_{-n} = -c_n$.

The autocorrelation of the input, $a(t - \lambda)$, is defined as

$$R_x(\sigma - \lambda) = \frac{1}{2T} \int_{-T}^{T} a(t - \lambda)\, a(t - \lambda - \sigma)\, dt. \qquad (4.2\text{-}6)$$

By comparison of the first term of (4.2-5) with (4.2-6), it is apparent that the first term of (4.2-5) can be written as

$$c_o R_x(\sigma - \lambda - t_o). \qquad (4.2\text{-}7)$$

With the changes of variable $\xi_1 = t - t_o - n\tau$, $\xi_2 = t - t_o + n\tau$ in the first and second integrals enclosed in the brackets of (4.2-5), respectively, these terms can be written as

$$\int_{-T-t_o-n\tau}^{T-t_o-n\tau} a(\xi_1 - \lambda)\, a(\xi_1 - \lambda - \sigma)\, d\xi_1 - \int_{-T-t_o+n\tau}^{T-t_o+n\tau} a(\xi_2 - \lambda)\, a(\xi_2 - \lambda - \sigma)\, d\xi_2. \qquad (4.2\text{-}8)$$

If

$$T \gg t_o + n\tau, \qquad (4.2\text{-}9)$$

(4.2-8) is approximately zero.

From (2.3-10), it is known that $c_{|n|} = 0$ for $n > t_o/\tau$ (where the $|n|$ in c_n follows from (2.3-9)). Thus, $n < t_o/\tau$ (i.e., $n\tau < t_o$) as regards computation of the terms (4.2-8). The condition (4.2-9) can be written as

$$T \gg t_o + t_o = 2t_o. \qquad (4.2\text{-}10)$$

In most practical systems (including Aerosat), this condition is met.

If the condition (4.2-10) prevails, it follows from the above that

$$R_y(\sigma - \lambda - t_o) \cong c_o R_x(\sigma - \lambda - t_o) \qquad (4.2\text{-}11)$$

That is to say that, if

a) The system is minimum-phase and symmetric in magnitude about ω_o ($|H(\omega_o + \Delta\omega)| = |H(\omega_o - \Delta\omega)|$) and

b) The input signal center frequency is equal to the system center frequency ($\omega = \omega_o$) and

c) Twice the center frequency is much greater than the bandwidth [$2\omega_o \gg (\omega_3 - \omega_2)$] and (4.2-12)

d) The integration time, 2T, is much greater than four times the midband group delay, $4t_o$ ($2T \gg 4t_o$),

the sole degradation of the autocorrelation signal due to nonlinear phase (only; recall that the effects of the magnitude response have not been considered) is expressible as (4.2-1). The constant c_o can be computed from (2.3-2):

$$c_o = \frac{1}{2\pi} \int_{-\pi}^{\pi} \cos\left[\frac{t_o''}{3!}(K\xi)^3 + \frac{t_o''''}{5!}(K\xi)^5 + \cdots + \frac{t_o^{(n-1)}}{n!}(K\xi)^n\right] d\xi \leq 1,$$

$$K = \frac{\omega_3 - \omega_2}{2\pi} = f_3 - f_2.$$

The above is not to say that one need not consider the effects of nonlinear phase on autocorrelation signals, but only that these should be considered from a different viewpoint than that which is conventionally employed.

First, arithmetic symmetry of the magnitude characteristic should be insured. One (of many) was of doing this is to bound $t_o^{(n)}$, n odd. Then, from (3.6-10), $t_o^{(n)}$, n even, should be bounded to minimize the signal loss (i.e., maximize c_o). "Differential group delay" becomes an obscure measure of performance.

If one equalizes, c_o more closely approaches unity but t_o is increased and, for the assumption (4.2-10) to hold, the integration time must be increased. The case for equalization, then, is not clear. In many practical autocorrelation systems of interest, there are, then, reasons <u>not</u> to equalize.

Prior to the formal development of the above theory, Mr. Robert Bland of the Department of Transportation's Transportation Systems Center (TSC) simulated ranging accuracy as a function of Aerosat Filter type [only minimum phase filters (Butterworth and Tchebyshev) were considered].[6] Although the effects of phase and amplitude distortions were not separated, Bland's results did suggest that, in accordance with the above, phase distortion, per se, had little effect on ranging accuracy.

LeFande[7] took a frequency-domain (as opposed to the present time-domain) approach to the present problem. His general conclusions are the same as those suggested by Bland's work and some preliminary computations of (4.2-13) (which indicate that $c_o \lesssim 1$ for a large class of filters); phase distortion is probably being "tightly" specified to an extent which does not justify the implied expense of equalization.

In many systems of practical interest (e.g., HF/SSB and telephone modems), the luxury of integrating over many signal "chips" is not afforded and the effects of differential group delay are more complicated and deleterious.

5.0 DISCUSSION AND COMPARISON WITH PREVIOUS WORK

That part c_{-n} of the result (2.3-9) is the same as that of Wheeler,[3] but that author considers only the lowpass case, thus obscuring the fact that the above is true only if arithmetic symmetry prevails. The fact that arithmetric asymmetry leads to AM to PM and PM to AM conversion is qualitatively stated by Panter.[4].

The work in Sections 3.2 (in-band amplitude ripple), and that in Sections 4.1 (differential group delay of the Aerosat wideband channel) and 4.2 (degradation of autocorrelation signals) are believed to be original. The latter results are believed to be more general than those stated by LeFande[6], as these do not depend on a specific signal format, but only on the method of detection. The former results are an extension of the work of Holmes and Keenan[1].

6.0 CONCLUSIONS

The principal conclusions of this work, stated in the order of their perceived importance, are

1) For any linear symmetric bandpass system meeting certain (practical) constraints, the output autocorrelation signal is related to the input autocorrelation signal by a constant which is less than one and greater than zero. This constant can be computed by the methods given in this work.
2) For both autocorrelation and "regular" signals, phase nonlinearity is best specified in terms of $t_o^{(n)}$, as opposed to Δt_{gr}.
3) For unequalized system transfer functions, the effects of in-band amplitude distortion on phase linearity can be computed by the methods of Section 3.2.

This (and other) work suggests that "tight" specification of phase distortion in systems wherein correlation detection is employed is unnecessary.

References

(1) T.R. Holmes and R.K. Keenan, "Numerical Results for Group Delay of Minimum Phase Bandpass Filters," IEEE Trans. Communication Technology, vol. COM-18, pp. 259-264, June 1970.

(2) W.J. Gill, "A Comparison of Binary Delay-Lock Tracking-Loop Implementations," IEEE Trans. Aerospace and Electronic Systems, vol. AES-2, No. 4, pp. 415-424, July 1966.

(3) H.A. Wheeler, "The Interpretation of Amplitude and Phase Distortion in Terms of Paired Echoes," Proc. IRE, vol. 27, pp. 359-385, June 1939.

(4) P.F. Panter, Modulation, Noise and Spectral Analysis, New York: McGraw-Hill, 1965, ch. 3.

(5) Handbook of Mathematical Functions with Formulas, Graphs, and Mathematical Tables. M. Abramowitz and I.A. Stegun, Ed., National Bureau of Standards, AMS-55, June 1964.

(6) R.G. Bland, Informal Communication, December 1975.

(7) R.A. LeFande, "Effects of Phase Nonlinearities on Phase-Shift-Keyed Pseudonoise Spread-Spectrum Communication Systems," IEEE Trans. Communication Technology, vol. COM-18, pp. 685-686, October 1970.

Appendix 1

Output of a Nonlinear Phase System

The purpose here is to derive the expressions (2.1-5) and (2.1-7). Towards this end, let

$$e^{-j\tilde{\theta}(\omega-\omega_o)} = \sum_{n=-\infty}^{\infty} c_n e^{j2\pi n(\omega-\omega_o)/(\omega_3-\omega_2)}, \qquad \omega_2 < \omega < \omega_3, \tag{A1-1}$$

where

$$c_n = \frac{1}{\omega_3 - \omega_2} \int_{\omega_2}^{\omega_3} e^{-j\tilde{\theta}(\omega-\omega_o)} e^{-j2\pi n(\omega-\omega_o)/(\omega_3-\omega_2)} d\omega. \tag{A1-2}$$

Then, from (2.1-2), that part of the frequency response due to system phase can be written as

$$e^{-j\theta(\omega)} = e^{-j[\theta_o + t_o(\omega-\omega_o)]} \sum_{n=-\infty}^{\infty} c_n e^{jn\tau(\omega-\omega_o)}, \tag{A1-3}$$

$$\tau = \frac{2\pi}{\omega_3 - \omega_2} = \frac{1}{f_3 - f_2}, \quad \omega_2 < \omega < \omega_3.$$

The impulse response of the phase box is the inverse Fourier transform of the frequency-domain response given in (A1-3):

$$h_\theta(t) = \sum_{n=-\infty}^{\infty} c_n e^{-j[\theta_o - \omega_o t_o - n\tau\omega_o]} \frac{1}{2\pi} \int_{-\infty}^{\infty} U(\omega) e^{-j\omega(t_o+n\tau)} e^{j\omega t} d\omega,$$

$$\omega_2 < \omega < \omega_3. \tag{A1-4}$$

where $U(\omega)$ is as given in Figure 2.1-1 and arises due to the finite interval (ω_2, ω_3) over which the Fourier expansion of $\tilde{\theta}(\omega - \omega_o)$ is postulated to be applicable.

Since multiplication in the frequency domain is equivalent to convolution in the time domain, (A1-4) can be written as

$$h_\theta(t) = \sum_{n=-\infty}^{\infty} c_n e^{-j[\theta_o - \omega_o t_o - n\tau\omega_o]} [u(t) \otimes \delta(t - t_o - n\tau)], \qquad \text{(A1-5)}$$

where $u(t)$ is the inverse Fourier transform of $U(\omega)$ and use has been made of

$$\frac{1}{2\pi} \int_{-\infty}^{\infty} e^{+j\omega(t-t_o-n\tau)} d\omega = \delta(t - t_o - n\tau). \qquad \text{(A1-6)}$$

The output of the phase box in response to an input $a(t)\, e^{j\omega t}$ is just the convolution of the input with the impulse response of the phase box:

$$\begin{aligned} y_\theta(t) &= x(t) \otimes h_\theta(t) \\ &= a(t)\, e^{j\omega t} \otimes \sum_{n=-\infty}^{\infty} c_n e^{-j[\theta_o - \omega_o t_o - n\tau\omega_o]} u(t) \otimes \delta(t - t_o - n\tau) \\ &= \left[\sum_{n=-\infty}^{\infty} c_n e^{j[\omega t - \theta_o + (\omega_o - \omega)(t_o + n\tau)]} a(t - t_o - n\tau) \right] \otimes u(t) \end{aligned} \qquad \text{(A1-6)}$$

where the order of convolutions has been changed and use has been made of the property $f(t) \otimes \delta(a) = f(a)$.

The output, $y(t)$, of the entire system (including the magnitude box) is just (A1-6) convolved with the impulse response of the magnitude box, $h_m(t)$:

$$y(t) = \left[\sum_{n=-\infty}^{\infty} c_n e^{j[\omega t - \theta_o + (\omega_o - \omega)(t_o + n\tau)]} a(t - t_o - n\tau) \right] \otimes u(t)$$

$$\otimes h_m(t)$$

$$= \tilde{y}_\theta(t) \otimes u(t) \otimes h_m(t) \qquad \text{(A1-7)}$$

$$= \tilde{y}_\theta(t) \otimes \mathcal{F}^{-1} \left| H(\omega) \right| U(\omega)$$

where

$$\tilde{y}_\theta(t) = \sum_{n=-\infty}^{\infty} c_n e^{j[\omega t - \theta_o + (\omega_o - \omega)(t_o + n\tau)]} a(t - t_o - n\tau) \qquad \text{(A1-8)}$$

The results (A1-6) and (A1-7) are those stated in (2.1-5) and (2.1-7) respectively.

Appendix 2

Group Delay Due To In-Band Amplitude Distortion

The initial purpose here is to derive the results (3.2-2) and (3.2-5). Towards this end, it is noted that, for a minimum-phase system, the phase is related to the amplitude characteristics by the Hilbert transform:[1]

$$\theta(\omega) = \frac{1}{\pi}\int_{\omega_2}^{\omega_3} \ln\left|\frac{\omega - x}{\omega + x}\right| \frac{d}{dx}\left[\ln \frac{|H(x)|}{|H(\omega_2)|}\right] dx, \qquad \omega_2 < \omega < \omega_3. \tag{A2-1}$$

Using Leibnitz' rule[5], the group delay is

$$t_{gr}(\omega) = \frac{d\theta(\omega)}{d\omega} = \frac{1}{\pi}\int_{\omega_2}^{\omega_3} \frac{\partial}{\partial\omega}\left\{\ln\left|\frac{\omega - x}{\omega + x}\right| \frac{d}{dx}\left[\ln \frac{|H(x)|}{|H(\omega_2)|}\right]\right\} dx, \tag{A2-2}$$

$$\omega_2 < \omega < \omega_3.$$

For the arbitrary amplitude distortion cited in (3.2-1),

$$\frac{d}{dx}\left[\ln \frac{|H(x)|}{|H(\omega_2)|}\right] = \sum_{n=1}^{\infty} \frac{\pi n b_n}{\omega_3 - \omega_2} \cos n\pi \left[\frac{x - \omega_2}{\omega_3 - \omega_2}\right], \tag{A2-3}$$

and (A2-2) becomes*

$$t_{gr}(\omega) = \sum_{n=1}^{\infty} \frac{n b_n}{\omega_3 - \omega_2}\left[\int_{\omega_2}^{\omega_3} \frac{1}{\omega - x} \cos n\pi \left[\frac{x - \omega_2}{\omega_3 - \omega_2}\right] dx - \int_{\omega_2}^{\omega_3} \frac{1}{\omega + x} \cos n\pi \left[\frac{x - \omega_2}{\omega_3 - \omega_2}\right] dx\right], \tag{A2-4}$$

$$\omega_2 < \omega < \omega_3.$$

* Removal of the magnitude sings in $|\omega - x|$ in (A2-2) has been effected by breaking the interval of integration, (ω_2, ω_3), into (ω_2, ω) and (ω_1, ω_3) so as to maintain $\omega - x$ or $x - \omega$ or $x - \omega$ positive quantities. The resulting integral is given in A2-4).

Now, both the variable x and the band of interest (in ω) is confined to (ω_2, ω_3). If this interval is small in comparison to ω_o $(= (\omega_3 + \omega_2)/2)$, the magnitude of the second integral in (A2.4) is on the order of $(\omega_2 - \omega_3)/2\omega_o$ times the magnitude of the first integral. Hereafter, it is assumed that

$$2\omega_o \gg (\omega_3 - \omega_2) \tag{A2-5}$$

and the second integral in (A2-4) is neglected.

With the change of variable $\xi = \omega - x$ in the first integral in (A2-4),

$$t_{gr}(\omega) \cong -\sum_{n=1}^{\infty} \frac{nb_n}{\omega_3 - \omega_2} \int_{\omega-\omega_2}^{\omega-\omega_3} \frac{1}{\xi} \cos n\pi \left[\frac{-\xi}{\omega_3 - \omega_2} + \frac{\omega - \omega_2}{\omega_3 - \omega_2}\right] d\xi,$$

$$\omega_2 < \omega < \omega_3, \qquad 2\omega_o \gg (\omega_3 - \omega_2). \tag{A2-6}$$

Using $\cos(x + y) = \cos x \cos y - \sin x \sin y$, (A2-6) can be written as

$$t_{gr}(\omega) \cong -\sum_{n=1}^{\infty} \frac{nb_n}{\omega_3 - \omega_2} \left[\cos n\pi \left(\frac{\omega - \omega_2}{\omega_3 - \omega_2}\right) \int_{\omega-\omega_2}^{\omega-\omega_3} \frac{1}{\xi} \cos \frac{n\pi\xi}{\omega_3 - \omega_2} d\xi \right.$$

$$\left. + \sin n\pi \left(\frac{\omega - \omega_2}{\omega_3 - \omega_2}\right) \int_{\omega-\omega_2}^{\omega-\omega_3} \frac{1}{\xi} \sin \frac{n\pi\xi}{\omega_3 - \omega_2} d\xi \right]. \tag{A2-7}$$

With the further change of variable

$$\lambda = \frac{n\pi\xi}{\omega_3 - \omega_2}, \tag{A2-8}$$

(A2-7) can be written as

$$t_{gr}(\omega) \cong -\sum_{n=1}^{\infty} \frac{nb_n}{\omega_3 - \omega_2} \left[\cos n\pi \left(\frac{\omega - \omega_2}{\omega_3 - \omega_2} \right) \int_{n\pi \frac{(\omega-\omega_3)}{(\omega_3-\omega_2)}}^{n\pi \frac{(\omega-\omega_2)}{(\omega_3-\omega_2)}} \frac{\cos\lambda}{\lambda} \, d\lambda \right.$$

$$\left. + \sin n\pi \left(\frac{\omega - \omega_2}{\omega_3 - \omega_2} \right) \int_{n\pi \frac{(\omega-\omega_2)}{(\omega_3-\omega_2)}}^{n\pi \frac{(\omega-\omega_3)}{(\omega_3-\omega_2)}} \frac{\sin\lambda}{\lambda} \, d\lambda \right] \qquad \text{(A2-9)}$$

By letting $\omega = \omega_o + \Delta\omega$, expanding the cos and sin functions (using well-known expressions for $\cos(x + y)$, $\sin(x + y)$) preceding the first and second integrals in (A2-9), respectively, and making use of, e.g.,

$$\cos n\pi/2 = \begin{cases} 0 & , \text{ n odd} \\ (-1)^{\frac{n}{2}+1} & , \text{ n even} \end{cases} \qquad \text{(A2-10)}$$

it can be shown from (A2-9) that

$$t_{gr}(\omega_o + \Delta\omega) \cong \sum_{n-1,\,3\ldots}^{\infty} \frac{(-1)^{\frac{n}{2}+1} nb_n}{(\omega_3 - \omega_2)} \left\{ \sin \frac{n\pi\Delta\omega}{\omega_3 - \omega_2} \int_{a-b\Delta\omega}^{-a+b\Delta\omega} \frac{\cos\lambda}{\lambda} \, d\lambda \right.$$

$$\left. - \cos \frac{n\pi\Delta\omega}{\omega_3 - \omega_2} \int_{a+b\Delta\omega}^{-a+b\Delta\omega} \frac{\sin\lambda}{\lambda} \, d\lambda \right\}$$

(A2-11)
(cont'd)

$$+ \sum_{n=2,4\ldots}^{\infty} \frac{(-1)^{\frac{n}{2}+1} n b_n}{\omega_3 - \omega_2} \left\{ \cos \frac{n\pi\Delta\omega}{\omega_3 - \omega_2} \int_{a+b\Delta\omega}^{-a+b\Delta\omega} \frac{\cos\lambda}{\lambda} \, d\lambda \right.$$

$$\left. + \sin \frac{n\pi\Delta\omega}{\omega_3 - \omega_2} \int_{a+b\Delta\omega}^{-a+b\Delta\omega} \frac{\sin\lambda}{\lambda} \, d\lambda \right\},$$

(A2-11 cont'd)

where

$$a = \frac{n\pi}{2}, \text{ and}$$

$$b = \frac{n\pi}{\omega_3 - \omega_2}. \qquad \text{(A2-12)}$$

No approximation other than (A2-5) has been made in deriving the above result.

Reduction of (A2-11) to (3.2 - 2) is straight forward.

In the arithmetically symmetric case, $b_n = o$, n even, and the terms following the second Σ are zero. Then, it follows from the above that

$$t_{gr}(\omega_o - \Delta\omega) = t_{gr}(\omega_o + \Delta\omega). \qquad \text{(A2-25)}$$

This is the result stated in (2.3-5). Finally, it should be noted that in present development, the interval (ω_2, ω_3) has not been restricted to the "bandpass" or any other segment of the response of a system. Therefore, the aforementioned results are generally applicable.

Appendix 3

Fourier Expansion of In-Band Amplitude Distortion

If the in-band amplitude distortion

$$F(\omega - \omega_2) = \ln\left[\frac{|H(\omega)|}{|H(\omega_2)|}\right] \tag{A3-1}$$

has a period twice the interval (ω_2, ω_3) and is odd about ω_2 (*i.e.*, $F(\omega - \omega_2) = -F(\omega_2 - \omega)$),

$$F(\omega - \omega_2) = \sum_{n=1}^{\infty} b_n \sin n\pi\left(\frac{\omega - \omega_2}{\omega_3 - \omega_2}\right), \tag{A3-2}$$

where

$$b_n = \frac{1}{2(\omega_3 - \omega_2)} \int_{2\omega_2 - \omega_3}^{\omega_3} F(\omega - \omega_2) \sin n\pi\left(\frac{\omega - \omega_2}{\omega_3 - \omega_2}\right) d\omega. \tag{A3-3}$$

But,

$$\int_{2\omega_2 - \omega_3}^{\omega_3} [\cdots] = \int_{2\omega_2 - \omega_3}^{\omega_2} [\cdots] + \int_{\omega_2}^{\omega_3} [\cdots] \tag{A3-4}$$

where $\cdots$ indicates the kernel of (A3-3). Since $F(\omega - \omega_2)$ is odd,

$$\int_{2\omega_2 - \omega_3}^{\omega_2} [\cdots] = \int_{\omega_2}^{\omega_3} [\cdots], \tag{A3-5}$$

so that

$$b_n = \frac{1}{\omega_3 - \omega_2} \int_{\omega_2}^{\omega_3} F(\omega - \omega_2) \sin n\pi \frac{\omega - \omega_2}{\omega_3 - \omega_2} \, d\omega. \qquad \text{(A3-6)}$$

This is given in (3.2-1a).

Since (A3-2) is an adequate representation of $F(\omega - \omega_2)$ in the interval $(2\omega_2 - \omega_3, \omega_3)$, it is an adequate representation of $F(\omega - \omega_2)$ in the lesser interval (ω_2, ω_3). Thus, (A3-2) is used to represent $F(\omega - \omega_2)$ and is applied in the bandpass interval (ω_2, ω_3) only.

Appendix 4

Noise Bandwidth of an Idealized Filter

The purpose here is to prove the result (4.1-1). This is applicable to a system with the characteristics shown in Figure 1.0-1 with a flat in-band response and

$$\Omega = \omega_4 - \omega_3 = \omega_2 - \omega_1 \tag{A4-1}$$

In the region $\omega_1 < \omega < \omega_2$,

$$\ln |H(\omega)| = \ln |H(\omega_1)| - \frac{\omega - \omega_1}{\Omega} \ln \left[\frac{|H(\omega_1)|}{|H(\omega_2)|} \right] \tag{A4-2}$$

or

$$|H(\omega)| = |H(\omega_1)| e^{a[\omega - \omega_1 / \Omega]} \tag{A4-3}$$

where

$$a = \ln \left[\frac{|H(\omega_2)|}{|H(\omega_1)|} \right] \tag{A4-4}$$

Similarly, in the region $\omega_3 < \omega < \omega_4$,

$$|H(\omega)| = |H(\omega_2)| \, e^{-a[\omega - \omega_3 / \Omega]} \tag{A4-5}$$

Because a is chosen to be large in the numerical example, the contribution to the noise bandwidth in the regions $\omega > \omega_4$ and $\omega < \omega_1$ is neglected; this amounts to neglecting contributions to the noise bandwidth which lie outside of the 60dB points of a practical apprximation of the idealized magnitude characteristic considered.

With the above assumption, the noise bandwidth is

$$N \cong \frac{1}{\left|H(\omega_2)\right|^2}\int_0^\infty |H(\omega)|^2\, d\omega = \frac{\left|H(\omega_1)\right|^2}{\left|H(\omega_2)\right|^2}\int_{\omega_1}^{\omega_2} e^{2a[\omega-\omega_1/\Omega]}\, d\omega$$

$$+\int_{\omega_2}^{\omega_3} d\omega + \int_{\omega_3}^{\omega_4} e^{-2a[\omega-\omega_3/\Omega]}\, d\omega. \qquad \text{(A4-6)}$$

By carrying out the integrations above, this is readily shown to be

$$N \cong (\omega_3 - \omega_2) + \frac{\Omega}{a}, \qquad \frac{\left|H(\omega_1)\right|}{\left|H(\omega_2)\right|} \ll 1. \qquad \text{(A4-7)}$$

This is the result given in (4.1-1).

25356